

Date of revision: 31 July 2013

Title: **2D THERMAL RESISTANCE OF PILE HEAT EXCHANGERS**

Authors: Fleur Loveridge<sup>a</sup>, William Powrie<sup>b</sup>

- a. Research Fellow  
Faculty of Engineering & the Environment,  
University of Southampton, Highfield, Southampton, SO17 1BJ  
United Kingdom  
Fleur.Loveridge@soton.ac.uk
- b. Professor of Geotechnical Engineering and Dean of the Faculty of  
Engineering and the Environment, University of Southampton,  
Faculty of Engineering & the Environment,  
University of Southampton, Highfield, Southampton, SO17 1BJ  
United Kingdom  
wp@soton.ac.uk

Corresponding Author: Dr Fleur Loveridge  
Faculty of Engineering & the Environment,  
University of Southampton, Highfield, Southampton, SO17 1BJ  
United Kingdom  
Tel: 0044 (0)7773346203  
Fax: 0044 (0)23 8067 7519  
Fleur.Loveridge@soton.ac.uk

Words in main text 6720

Tables 5

Figures 12

## **2D thermal resistance of pile heat exchangers**

### **Abstract**

Structural foundation piles are being used increasingly as heat exchangers to provide renewable heat for new buildings. To design such energy systems a steady state is assumed within the pile, which is conventionally characterised by constant thermal resistance. However, there has been little research regarding pile resistance and there are few published case studies. Numerical modelling results are presented here to provide typical values of pile resistance, depending on the details of the heat exchange pipes. Analysis suggests large diameter piles may take several days to reach steady state; in these cases a transient design approach may be more appropriate. (100 words)

**Keywords:** geothermal, piled foundations, ground energy, thermal resistance, ground heat exchangers

## Notation

### Main symbols

c	concrete cover to pipework (m)
d	diameter (m)
h	heat transfer coefficient
L	characteristic length, usually 2r for pipes or heat exchangers
n	number of pipes
Nu	$\frac{hL}{\lambda_{fluid}}$ Nusselt number (ratio of convective to conductive heat transfer)
Pr	$\frac{\nu}{\alpha}$ Prandtl number (ratio of viscous diffusion rate to thermal diffusion rate)
q	heat flux (W/m)
R	thermal resistance (mK/W)
R <sub>a</sub>	internal thermal resistance of borehole or pile (mK/W)
R <sub>b</sub>	thermal resistance of borehole or pile (mK/W)
R <sub>c</sub>	thermal resistance of concrete (mK/W)
R*	effective thermal resistance of borehole or pile, including the effects of pipe to pipe interactions (mK/W)
Re	$\frac{uL}{\nu}$ Reynolds number (ratio of inertial to viscous forces for fluid flow)
r	radius (m)
S <sub>b</sub>	Remund's shape factor for borehole heat exchangers
S <sub>c</sub>	shape factor for concrete in pile heat exchangers
s	shank spacing (m)
T	temperature (°C or K)
u	fluid mean velocity (m/s)
$\alpha$	thermal diffusivity (m <sup>2</sup> /s)
$\lambda$	thermal conductivity (W/mK)
$\nu$	kinematic viscosity (m <sup>2</sup> /s)

### Subscripts

b	borehole or pile
c	concrete
ff	far field
g	ground
i	inner dimension of pipe
o	outer dimension of pipe
p	pipe
steady	steady state heat flow
trans	transient heat flow

## 1 Introduction

Closed loop ground energy systems, with heat exchange pipes embedded in the ground, have long been recognised as a potentially sustainable means of providing heating and cooling to buildings. Systems typically comprise vertical drilled heat exchangers or horizontal “slinky” type pipe installations depending on the land available and the building thermal loads. Recently there has been an increase in the use of structural foundation piles as closed loop vertical heat exchangers (Amis, 2009). In this case the heat exchanger pipes are typically fixed to the structural pile steel reinforcement cage prior to placing the cage in the pile bore and concreting (Figure 1a). Alternatively for contiguous flight auger (CFA) type piles, the pipes may be plunged into the centre of the pile bore after placing the concrete (Figure 1b). Despite the increased use of pile heat exchangers, often termed thermal piles, research into their behaviour has been limited compared with other types of ground heat exchanger (Loveridge & Powrie, 2013). Consequently uncertainties remain about design methods and parameter selection.

Conventional design of closed loop pile heat exchangers typically separates the internal (ie within the heat exchanger) and the external (ie within the ground) thermal response of the system. The pile element is usually assumed to be at an instantaneous steady state as far as internal heat transfer between the thermal fluid and the exterior surface of the concrete is concerned. While the temperature of the pile may vary with time, it is usually assumed that the pile surface temperature is constant around the circumference and along the length of the pile at any point in time. However, this simplification, while making analysis more straightforward, does not represent real behaviour.

This paper investigates, by means of numerical analyses, heat transfer within a pile and at the concrete surface, and how this varies depending on the number of heat exchange pipes and the depth of concrete cover. The results of the analyses are then used to define the limits of validity of the conventional design assumptions listed above, and to propose an empirical equation to allow calculation of the temperature difference between the fluid and the ground.

## 2 Background

Design approaches for closed loop vertical ground energy systems typically assume that the heat exchanger is at thermal steady state based on a two dimensional slice through the heat exchanger. The temperature change between the fluid in the pipes and the edge of the heat exchanger ( $\Delta T$ ) can then be calculated on the basis of the resistance of the heat exchanger,  $R_b$ .

$$R_b = \frac{\Delta T}{q} \quad \text{Equation 1}$$

where  $q$  is the heat transfer rate per unit length of the heat exchanger and  $R_b$  is the resistance. Thermal resistance depends on both the material property (thermal conductivity) and the heat flow path lengths, which in turn depends on the object geometry and the distribution of the temperature at the boundaries.  $\Delta T$  in Equation 1 is the temperature difference between the source and sink, ie between the fluid and the edge of the concrete heat exchanger. It is common to assume that the temperature at these boundaries is, at a given time, uniform. However, in some cases (eg constant

applied heat flux to a solid object) this is not the case. In such cases it is appropriate to use a mean value of the temperature, but a different value of  $R_b$  will result (Incropera et al, 2007), owing to changes in the heat flow path geometry.

This approach assumes that the heat transfer within and around the heat exchanger is principally occurring in the horizontal plane. However, three dimensional effects do occur as the result of the vertical movement of the heat transfer fluid within the pipes and the potential for pipe to pipe interactions. If these effects are significant they will act to increase the effective or three dimensional thermal resistance, known as  $R_b^*$ . The factors controlling  $R_b^*$  are the 2D resistance  $R_b$ , the internal resistance between the heat transfer pipes,  $R_a$ , the length of the pipe circuit within the heat exchanger and the fluid flow rate.  $R_b$  is the most important of these factors (Anstett et al, 2005) and will be the main focus of this paper.

For drilled borehole heat exchangers there has been significant research regarding methods for determining  $R_b$  (eg Hellstrom, 1991; Lamarche et al 2010; Remund, 1999), in addition to well documented case studies and published typical values based on in situ testing (eg Table 1). However, the corresponding database of both experience and research has yet to be fully developed for pile heat exchangers and there is an absence of reliable guidance for designers in selecting values of thermal resistance for use in design. The following sections of this paper review existing approaches for determining  $R_b$  for vertical heat exchangers, and the key parameters influencing the result. Sections 3 and 4 present numerical modelling data which explore the importance of the different parameters and challenge some of the assumptions behind the simpler analytical design approaches which are commonly adopted. While the scope of the analysis is restricted to the two dimensional resistance  $R_b$ , Section 5 includes some discussion of the other factors which will influence the effective resistance  $R_b^*$ , including comments on the likely magnitude of pipe to pipe interaction effects. Section 6 then compares the results obtained by this study to published case study data.

**Table 1 Typical Values of Borehole Thermal Resistance based on in situ Testing (after Sanner et al , 2005)**

Boreholes	Grout	Thermal Resistance (mK/W)
100 to 200 mm diameter	Standard	0.10 – 0.20
	Thermally Enhanced	0.06 – 0.10

## 2.1. Analytical Approaches

2D thermal resistance for vertical ground heat exchangers is usually expressed as the sum of its component parts:

$$R_b = R_{pconv} + R_{pcond} + R_c \quad \text{Equation 2}$$

where the subscripts  $p$  and  $c$  refer to the pipe and concrete (or grout).  $R_{pconv}$  and  $R_{pcond}$ , the resistances associated with the flowing fluid and the pipe material respectively, usually represent the effects of a number of individual pipes operating in parallel.

Assuming a spatially uniform pipe wall temperature,  $R_{pconv}$  is usually calculated using the following expression:

$$R_{p_{conv}} = \frac{1}{2n\pi r_i h_i} \quad \text{Equation 3}$$

where  $n$  is the number of pipes within the heat exchanger cross section,  $r_i$  is the pipe internal radius and  $h_i$  is the heat transfer coefficient. The Nusselt number can be used to calculate  $h_i$ ; for turbulent flow the most common expression for this is the Dittus-Boelter equation, which gives:

$$h_i = \frac{Nu\lambda_{fluid}}{2r_i} = \frac{0.023Re^{0.8} Pr^{0.35} \lambda_{fluid}}{2r_i} \quad \text{Equation 4}$$

The pipe conductive resistance can be assessed using the equation for the resistance of a hollow cylinder with constant temperature boundaries on the inner and outer surfaces. For  $n$  pipes in parallel:

$$R_{p_{cond}} = \frac{\ln(r_o/r_i)}{2n\pi\lambda_{pipe}} \quad \text{Equation 5}$$

where  $r_o$  is the outer radius of the pipe.

The concrete or grout resistance is more difficult to assess and a number of methods have been adopted for borehole heat exchangers. The first (eg Shonder & Beck, 2000) considers the material as an equivalent hollow cylinder with the outer radius taken to be the heat exchanger radius  $r_b$  and an inner effective radius,  $r_{eff}$ , determined as follows:

$$r_{eff} = r_o \sqrt{n}$$

The concrete resistance then becomes:

$$R_c = \frac{\ln(r_b/r_{eff})}{2\pi\lambda_c} \quad \text{Equation 6}$$

To apply the analytical solution for the thermal resistance of a cylinder it is assumed that at a given point along the length of the heat exchanger the outside of the cylinder is at a uniform temperature. Although that temperature may vary with time and with depth, around the circumference it must be constant. In reality, this is not necessarily the case for vertical heat exchangers, and the significance of a variable circumferential temperature will be explored later in section 4 of this paper. Also the equivalent cylinder approach takes no account of the actual positioning of the pipes, specifically their offset from the edge of the heat exchanger and their distance from each other. Consequently, unless the pipes are in contact with each other at the centre of the hole, Equation 6 will overestimate the 2D thermal resistance (Sharqawy et al, 2009).

The second method, developed by Remund (1999), uses an empirically derived shape factor,  $S_b$ , to determine  $R_c$ . Values of  $R_c$  were determined experimentally from field tests of borehole heat exchangers with three configurations of two pipes (Table 2). Shape factors were then back calculated from the measured values of  $R_c$  (Equation 7) and an empirical equation for  $S_b$  was derived (Equation 8).  $S_b$  depends on the ratio of

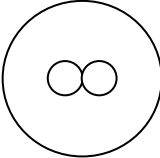
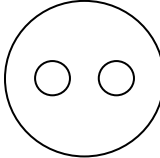
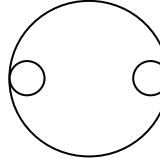
the borehole and pipe radii and two empirical constants  $\beta_0$  and  $\beta_1$ . The values of the constants for the different pipe configurations are given in Table 2.

$$R_c = \frac{1}{S_b \lambda_{grout}} \quad \text{Equation 7}$$

$$S_b = \beta_0 \left( \frac{r_b}{r_o} \right)^{\beta_1} \quad \text{Equation 8}$$

The disadvantage of Remund's approach is that it can be difficult to know accurately the positions of the installed pipes. It is also not applicable to most pile heat exchangers, which are installed with more than one pair of pipes.

**Table 2 Borehole heat exchanger configurations (after, Remund, 1999)**

	Configuration A Shanks central and touching	Configuration B Intermediate position of equal shank spacing	Configuration C Shanks touching borehole edge
			
$\beta_0$	20.10	17.44	21.91
$\beta_1$	-0.9447	-0.6052	-0.3796

The most rigorous method of determining  $R_c$  is to assume that each pipe is a line heat source or a multi-pole (a complex number derivative of a line source) and then use superposition to determine exactly the heat flux related to each pipe and hence the overall resistance. The multi-pole method (Bennet et al, 1987) is very powerful and a review by Lamarche et al (2010) showed that it provided the best match to numerical simulations of heat transfer within borehole heat exchangers. However, precise internal geometry information is required to make such calculations and the mathematical approach is complex. Relatively simple expressions can be derived for two pipe systems (Hellstrom, 1991). These are included in Appendix A, but they will not be suitable for most pile heat exchangers which contain more than one pair of pipes.

## 2.2. Factors Affecting Thermal Resistance of the Concrete

If the temperature around the pile circumference is constant, it is apparent from Equations 6 to 9 that the two factors controlling  $R_c$  are the concrete thermal conductivity,  $\lambda_c$  and the concrete geometry, ie the size and arrangement of the pipes relative to the pile cross section. The constituents of concrete have widely differing thermal conductivities (Table 3), and overall thermal conductivity depends mainly on the aggregate lithology, aggregate volume ratio and water content (Tatro, 2006). Concrete piles installed in clay soils or in any geological conditions below the water table are likely to be saturated. Neville (1995) reports typical values of saturated concrete thermal conductivity between 1.4 W/mK and 3.6 W/mK. However, the more conductive concrete mixes will be those with a high volume ratio of aggregates. Since foundation concrete is of high strength it will have a smaller proportion of aggregates and hence be at the lower end of this thermal conductivity range. Piles installed in dry

sands may have a lower thermal conductivity owing to the reduced water content. The use of cement replacement products can also lead to a reduction in thermal conductivity by up to 20% (Kim et al, 2003).

**Table 3 Typical Thermal Conductivities of Materials**

Material	Typical Thermal Conductivity (W/mK)
Neat cement	0.3 – 0.6
Saturated concrete	1.4 – 3.6
Air	0.024
Water	0.6
Sandstone	3 – 3.5
Limestone	2.5
Clay	1.0 – 1.5

If, however, the temperature of the concrete at the edge of the heat exchanger varies around the circumference, as is the case in most real scenarios, the thermal resistance will also be affected by the thermal conductivity of the surrounding ground (as reflected in Equations A1 and A2). This is because the heat flow paths are altered by the non-uniform temperature around the circumference. The thermal conductivities of soils and rocks fall within a similar range to concrete with typical values between 1 W/mK for dry clay soils up to about 3.5 W/mK for saturated quartz rich formations such as sandstones (Banks, 2008; Cote & Konrad, 2005). As with concrete, replacement of air within the pore-spaces by water will increase the thermal conductivity.

The geometric arrangement of the heat exchanger pipes is usually well known, if they are fixed to the pile steel reinforcement cage and controlled within standard construction tolerances. As pile reinforcement must be protected from corrosion there tends to be a greater concrete cover to the pipes than with borehole heat exchangers. This can lead to a greater resistance. On the other hand, the likely increased number of pipes within the cross section would tend to reduce the resistance. However, if the pipes are too closely spaced thermal interactions can occur, reducing the efficiency of heat transfer and hence increasing the effective thermal resistance (Loveridge & Powrie, 2013). This tends to be exacerbated at low fluid flow rates.

### 3 Pile Only Model

To investigate the effects of the number and arrangement of pipes on the concrete thermal resistance of pile heat exchangers, two-dimensional heat transfer models have been set up using the finite element software COMSOL (version 4.1, COMSOL, 2010). The programme solves the diffusion equation for a given pile geometry and boundary conditions. Figure 2a shows a schematic layout for the steady state model with pipes installed with a concrete cover,  $c$ , from the edge of the pile. The pipes are equally spaced around the pile circumference, and the distance between pipe centres measured across the pile is the shank spacing,  $s$ . Constant temperatures  $T_b=20^\circ\text{C}$  and  $T_p=10^\circ\text{C}$  are applied at the pile edge and the pipe surface boundaries respectively.

The model domain is restricted to the pile concrete (assumed to be homogeneous); the pipe material and fluid are not modelled. This means that the model can only determine the concrete resistance  $R_c$  and that the pipe resistances  $R_{p\text{cond}}$  and  $R_{p\text{conv}}$  are



neglected. These are both straightforward to calculate and providing flow is turbulent are typically lower in value than  $R_c$  and hence less significant. The concrete domain was meshed using triangular elements of a maximum size of 2mm at the pipe boundary and 10mm at the pile edge. Steady state analyses were carried out using a stationary PARDISO solver assuming constant temperatures at pipe and pile circumference.

For the case considered, the thermal resistance will depend only on the geometry of the problem and the thermal conductivity. It will not be influenced by the temperatures imposed or the magnitude of the heat fluxes resulting from the temperature differences. To separate the geometry and thermal conductivity components of the resistance, the results of the model analyses are presented in terms of a shape factor,  $S_c$ , where:

$$R_c = \frac{1}{\lambda_c S_c} \quad \text{Equation 9}$$

The shape factor was determined as:

$$S_c = \frac{\sum_{i=1}^{i=n} q_{p(i)}}{\lambda_c (T_b - T_p)} \quad \text{Equation 10}$$

where  $q_{p(i)}$  is the calculated heat flux along a single pipe circumference and there are  $n$  pipes in the model. The model and mesh resolution were validated by considering a 600mm diameter pile heat exchanger with only one pipe installed (Figure 2b). The results for this case were checked against Equation 11, the analytical solution for an eccentric cylinder (Incropera et al, 2007). The mesh was refined until the difference between Equations 10 and Equation 11 was less than 0.2%.

$$S_c = \frac{2\pi}{\cosh^{-1}\left(\frac{4r_b^2 + 4r_{ro}^2 - s^2}{8r_b r_{ro}}\right)} \quad \text{Equation 11}$$

During each analysis the heat flux across the pile circumference ( $q_b$ ) was also checked against the heat flux for the pipe surfaces:

$$q_b = \sum_{i=1}^{i=n} q_{p(i)} \quad \text{Equation 12}$$

The error was consistently less than 0.3% in all analyses.

Some additional error is introduced into the analysis by the simplified boundary conditions used within the model. The movement of the heat transfer fluid through the pipes will result in a spatially non uniform heat flux around the pipe wall circumference. However, sensitivity analyses suggest that this variation in the heat flux leads to only a small spatial variation in the pipe wall temperature. Moreover the difference in the values of shape factor and thermal resistance resulting from these temperature variations is of the same order of magnitude as the errors resulting from the numerical discretisation. Consequently this simplification is considered of negligible significance compared with the overall result. The consequence of

excluding the ground domain and assuming a constant temperature around the pile circumference is of greater impact and this is investigated in Section 4.

### 3.1. Results

The model was used to calculate the shape factors for a number of different pile and pipe geometries. The full range of results is tabulated in Appendix B and selected results are shown in Figure 3 to illustrate important trends. The range of theoretical shape factor values is wide; from 2 to 20. This gives equivalent resistance values from ~0.02 mK/W to ~0.3 mK/W, depending on the thermal conductivity of the concrete. The results of the analyses are discussed in more detail below. Except where specifically indicated in the text, the pipes were always arranged symmetrically, corresponding to their having been fixed to the pile steel reinforcement in a controlled manner.

#### 3.1.1 *Effect of Number of Pipes and Concrete Cover*

Figure 3a shows the shape factors and thermal resistances calculated for a typical 600mm diameter heat exchanger pile with 25mm diameter pipes installed. It can be seen that the number of pipes installed and their concrete cover,  $c$ , have a large influence. The shape factor increases (and the resistance reduces) with the number of pipes and as the cover is reduced. However, the increase in the shape factor starts to diminish as greater numbers of pipes are installed. The range of values of shape factor is greatest when the cover is small. This range is significantly reduced where the cover is greatest. Consequently, there is minimal benefit from installing more than two pipes in such cases.

Figure 3b shows the shape factors for a 600mm CFA pile where the pipes are attached to a 40mm steel bar for installation, giving a concrete cover of 255mm. As it is difficult to control whether the pipes are evenly spaced in a CFA pile, the effect of all the pipes being bunched together was investigated. The results show a small reduction in the shape factor when the pipes are not symmetrical, but this is minor compared with the other factors discussed above. Thus the number and arrangement of pipes is less important for CFA or other piles with substantial concrete cover to the pipes.

#### 3.1.2 *Effect of Pipe and Pile Size*

A parametric study was carried out for three pile diameters ( $2r_b=300$  mm, 600 mm and 1200 mm) and three pipe sizes ( $2r_o=20$  mm, 25 mm and 30 mm) for a range of concrete cover depths  $c$ . The results are tabulated non-dimensionally in Appendix B in terms of the ratios  $r_b/c$  and  $r_b/r_o$ . Larger values of  $r_b/c$  and smaller values of  $r_b/r_o$  (for equal  $r_b/c$ ) give the largest shape factors and hence the smallest resistances. Thus smaller pile diameters typically give larger shape factors. However, larger piles with many pipes are also associated with large values of shape factor when the ratio  $r_b/c$  is high, ie for large diameter piles with small cover.

In fact, if the resistance is normalised against the diameter of a 1200mm diameter pile, then larger diameter piles are seen to be advantageous when the pipes can be installed near the pile edge. Figure 4a shows the concrete resistance of different size piles and the total resistance for an imaginary outer diameter of 1200mm. To calculate the total resistance for this case the resistance of an additional ring of soil (using the analytical expressions applied in Equations 5 and 6) was added to the concrete resistance determined from the model. This shows that for a given number of pipes the concrete

resistance is similar regardless of the diameter. However, when an equivalent diameter is considered the larger diameter piles have much lower resistance.

Interestingly, a reverse pattern is seen for CFA type piles which have pipes installed in the centre. Figure 4b shows both the concrete resistance for CFA piles and for a total equivalent diameter of 1200mm. In this case the resistance is larger for larger diameter piles, but is equalised when the total resistance at the equivalent diameter is considered. In all cases the total resistance is more for CFA pipes compared with the case with pipes installed near the pile edge. This exercise shows the benefit in using large diameter piles for heat exchangers, providing the pipes can be installed near the edge of the pile.

### 3.1.3 Comparison with Analytical and Empirical Solutions

For the special case of only two pipes installed the calculated shape factors may be compared with analytical and empirical methods developed for borehole heat exchangers. Figure 5 compares the results for a 600mm diameter pile with  $r_o=25\text{mm}$  to the three methods described in Section 2 and also the empirical Equation 13 derived by Sharqawy et al (2009) based on numerical modelling of borehole heat exchangers. Sharqawy et al (2009)'s 2D steady state model is similar to that presented in this paper, but for different geometries.

$$R_c = \frac{1}{2\pi\lambda_c} \left[ -1.49 \left( \frac{s}{2r_b} \right) + 0.656 \ln \left( \frac{r_b}{r_o} \right) + 0.436 \right] \quad \text{Equation 13}$$

It can be seen from Figure 5 that the simple equivalent cylinder approach (Equation 6) always underestimates the shape factor (overestimates the resistance), with the difference being greatest when the cover is smaller. Of the three scenarios proposed by Remund (1999), Case B gives a similar result to that for a pile with a large concrete cover. The empirical equation of Sharqawy et al (2009) provides a better approximation to the shape factor as it takes into account changes in cover through the shank spacing term,  $s$ , in Equation 13. The closest match is provided by the line source equation (Equation 14, Hellstrom, 1991). For the special case where the ground and concrete have the same thermal conductivity then the line source and first order multipole equations reduce to the same simple expression:

$$R_c = \frac{1}{4\pi\lambda_c} \left[ \ln \left( \frac{r_b}{r_o} \right) + \ln \left( \frac{r_b}{s} \right) \right] \quad \text{Equation 14}$$

The key difference between Equation 13 and Equation 14 is that the shank spacing to pile radius ratio appears non-linearly in Equation 14. Equation 14 provides a much better fit to the modelled pile heat exchanger data, especially for large values of concrete cover ( $r_b/c \leq 3$ ). However, there are still discrepancies of up to 18% at smaller values of concrete cover. This is because the numerical model imposes a uniform temperature around the pile circumference, whereas the line source equation does not include this restriction (Hellstrom, 1991). For  $r_b/c < 2$  the nature of the circumferential temperature distribution appears not to be significant, but errors in the steady state model increase as the pipes get closer to the edge of the pile. To improve accuracy in this respect, transient analysis is required; this is discussed in Section 4.

## 4 Extended Pile and Ground Model

In most cases the temperature around the circumference of the pile will vary spatially as opposed to being constant as assumed in the pile only model described in Section 3 (Figure 2). To investigate the importance of this, a two dimensional transient heat transfer model was created. The model domain is now extended to include the ground surrounding the pile out to a radial distance of 25m. This is sufficient for the influence of the boundary on the heat transfer around and within the pile to be negligible. Constant temperatures were imposed at the pipe boundaries as before ( $T_p=10^\circ\text{C}$ ) and also at the new outer far field boundary ( $T_{ff}=20^\circ\text{C}$ ). The mesh was generated on the same basis as the pile only model, except that the element size expands from the pile edge towards the farfield boundary. The analyses were carried out using a time dependent backward differentiation formula (BDF) solver.

The temperature at the pile circumference, for use in calculating  $R_c$  and the shape factor, was determined from the results of the transient analysis. An integral mean value of temperature was used to allow for the fact that the temperature is now no longer uniform around the pile circumference. As both the heat flux from the pipes and the pile circumferential temperature also change with time, the shape factor was calculated dynamically as a function of time using Equation 10 and the analysis continued until an asymptotic value of the steady state shape factor was approached. For the purpose of the analysis, the asymptotic value was chosen as the calculated shape factor when this value did not change by more than  $10^{-4}$  over a time period of one day.

### 4.1. Results

Full results from the analysis are presented as dimensionless look up tables in Appendix B. For a 600mm diameter pile with two pipes of diameter  $2r_o=25\text{mm}$ , Figure 6 compares the pile only shape factor derived in Section 3 with the results from the extended pile and ground model asymptotic shape factor. In this case the simpler model overestimates the shape factor by as much as 10% to 25% when the concrete cover is small. The error reduces as the cover increases and as suggested in Section 3.1.3, the effect becomes insignificant for  $r_b/c \leq 2$ .

The shape factor results depend on the ratio of the ground and concrete thermal conductivities as well as the concrete cover depth (Figure 6). As an asymptotic steady state shape factor is being calculated, the thermal diffusivity does not effect the outcome, only the time taken for the model to reach a steady state (see also Section 4.5). Variations in thermal conductivity by up to a factor of two have been investigated; this can change the shape factor by  $\pm \sim 5\%$  compared with the case where the thermal conductivities of the ground and concrete are equal. Shape factors are larger and hence resistances smaller where the ground conductivity is greater than that of the concrete.

As indicated, the discrepancies between the two models are greatest when the concrete cover is smallest. This is consistent with the studies of Lamarche et al (2010) for boreholes, and arises because of the greater degree of temperature variation around the pile circumference at any given time. Figure 7a shows example circumferential temperatures changes from the pile and ground model when the pile has reached steady state. As the pipes become closer to the centre of the pile, the temperature of the circumference approaches a constant value. Similarly, as shown in

Figure 7b, if more pipes are installed there will be less variation in the temperature at the circumference.

Both points are also illustrated in Figure 8, which shows the percentage difference in shape factor calculated using the two models for the case where the concrete and ground have the same thermal conductivity. The difference between the ground only and the pile and ground model appears to be controlled mainly by the number of pipes and the pile radius to cover ratio  $r_b/c$ . Any influence of the pile to pipe radius ratio  $r_b/r_o$  appears much less significant. This is in contrast to borehole heat exchangers, for which  $r_b/r_o$  appears to be a more important parameter (Lamarche et al, 2010). This is likely to be because of the different ranges of this parameter;  $r_b/r_o \geq 10$  for piles, but is as low as 3 for boreholes.

#### 4.2. A new expression for thermal resistance of pile heat exchangers

Based on existing expression (Equations 13 & 14) the shape factor is known to be dependent on logarithmic relations with the non-dimensional parameters  $r_b/c$  and  $r_b/r_o$ . Through experimentation the results of the sensitivity analyses presented in Section 4.1 and Appendix B were found to be best represented by an equation of the form:

$$S_{c(steady)} = \frac{A}{B \ln\left(\frac{r_b}{r_o}\right) + C \ln\left(\frac{r_b}{c}\right) + \left(\frac{r_b}{r_o}\right)^D + \left(\frac{r_b}{c}\right)^E + F} \quad \text{Equation 15}$$

where A, B, C, D, E and F are constants determined by curve fitting and whose values depend on the number of pipes and the conductivity ratio, as shown in Table 4. The inclusion of different numbers of pipes in the analysis, rather than just 2 (as per Equations 13 & 14), leads to the inclusion of the additional power terms in Equation 15. The validity of the form of the equation was tested statistically and the coefficient of determination was  $>0.99$  in all cases. However, the residuals were found to vary, with the largest values being associated with the case of 8 pipes installed in the pile cross section. Figure 9 quantifies the resulting error in concrete resistance calculated using Equation 9 and Equation 15 compared with the numerical model. A range of realistic values of thermal resistance based on the results of this study are used to bound the output. It can be seen that the errors between the empirical equation and the model are typically of the order of a few percent, but are larger when the resistance is greater and where there are more pipes installed. However, in reality, a situation with 8 pipes in the cross section and a resistance  $>0.2$  mK/W is unlikely to occur. Therefore, the errors in determining  $R_c$  using Equation 15 are likely to be less than 5% compared with the numerical model. Limitations to this approach which may result in other sources of error are discussed in Section 5 & 6.

**Table 4 Curve fitting results for the pile and ground model (Equation 15)**

	2 pipes			4 pipes			6 pipes			8 pipes		
	$\lambda_c=\lambda_g$	$\lambda_c=2\lambda_g$	$2\lambda_c=\lambda_g$	$\lambda_c=\lambda_g$	$\lambda_c=2\lambda_g$	$2\lambda_c=\lambda_g$	$\lambda_c=\lambda_g$	$\lambda_c=2\lambda_g$	$2\lambda_c=\lambda_g$	$\lambda_c=\lambda_g$	$\lambda_c=2\lambda_g$	$2\lambda_c=\lambda_g$
A	4.919	4.34	4.853	3.33	3.284	3.369	3.171	3.162	3.18	3.203	3.201	3.208
B	0.3549	0.317	0.345	0.1073	0.1051	0.1091	0.08526	0.08669	0.08386	0.0609	0.06157	0.05989
C	-0.07127	-0.001228	-0.1676	-0.07727	-0.05823	-0.09659	-0.07458	-0.06736	-0.08085	-0.06795	-0.06399	-0.06839
D	-11.41	-10.18	-16.76	-10.9	-11.98	-11.79	-1.28	-1.256	-1.304	-1.391	-1.378	-1.394
E	-2.88	-2.953	-3.611	-2.9	-2.782	-3.032	-2.743	-2.686	-2.791	-2.503	-2.466	-2.499
F	0.06819	-0.002101	0.1938	0.1278	0.1027	0.1535	0.05347	0.03534	0.06954	0.07836	0.06846	0.08188
R <sup>2</sup>	0.9985	0.9975	0.9987	0.9976	0.9971	0.9975	0.9991	0.9990	0.9992	0.9993	0.9993	0.9992
RMSE	0.033	0.044	0.035	0.120	0.130	0.126	0.117	0.123	0.113	0.132	0.137	
Typical value of residuals	<0.04	<0.06	<0.04	<0.15	<0.2	<0.2	<0.15	<0.15	<0.15	<0.15	<0.2	<0.2
Maximum value of residuals	0.06	0.09	0.08	0.22	0.27	0.37	0.31	0.32	0.30	0.42	0.43	0.48

#### 4.3. Comparison with line source and multipole equations

For the special case of two pipes, the results in Figure 6 have been compared with the line source and multi-pole equations given in Appendix A. The transient model shows less than 0.5% variation from the line source equation, which itself results in values within 0.1% of the first order multi-pole equation. Consequently, for energy piles with two pipes it is recommended that the line source equation is used to determine  $R_c$ . The additional accuracy gained from the more complex multi-pole equation does not appear to be justified.

For piles with more than one pair of pipes installed, Equation 15 has been compared with values of the total pile thermal resistance calculated using the multipole method and published by the Swiss Society of Engineers and Architects (Anstett et al, 2005). To make the results directly comparable  $R_{pconv}$  and  $R_{pcond}$  were added to the value of  $R_c$  determined using Equation 15. As these simulations assumed laminar flow a constant value of 3.66 was assumed for the Nusselt number (Hellstrom, 1991) calculating the heat transfer coefficient between the fluid and the pipe. Pipe conductivity was taken as 0.4 W/mK in keeping with Anstett et al (2005) and the fluid conductivity was assumed to be 0.6 W/mK.

Figure 10 shows the results of the multipole simulations assuming a concrete thermal conductivity of 1.8W/mK. Superimposed on this are total resistance values calculated using Equations 2, 3, 5 and 15, with the input parameters described above. This results in slightly larger values of resistance than calculated by the multipole method, by up to about 0.01mK/W or 10%. There are two potential sources for this discrepancy. Some errors may result from the curve fitting used to derive Equation 15. In addition it has been necessary to make an assumption regarding the thermal conductivity of the fluid which was not specified in Anstett et al (2005). Nonetheless the trends are well matched and as the new approach is conservative, the use of Equation 15 is considered a useful and simpler alternative to a full multipole simulation.

Figure 10 also confirms the trend shown in Figure 4, with piles of different diameters having similar resistance values providing the same numbers of pipes are installed. However, larger diameter piles provide greater opportunities to install more pipes, without risking significant pipe to pipe interactions (see Section 5) and thus have the potential for reduced total thermal resistance.

#### 4.4. Time to Achieve Steady State

As design methods for pile heat exchangers (eg Pahud, 2007) usually assume that the pile concrete is at a thermal steady state, the time to achieve this has been determined from the analysis. For practical purposes the definition of steady state could be less rigorous than the criterion adopted for the asymptotic value of the shape factor presented in Section 4.1 and Appendix B. Therefore the time to achieve steady state has been assessed as when 98% of the asymptotic value of  $R_c$  (as calculated by Equation 10) has been reached.

Figure 11 shows the range of times taken for the piles to reach steady state assuming a thermal diffusivity of the ground and concrete of  $1.25 \times 10^{-6} \text{ m}^2/\text{s}$ . This is at the high

end of the range of concrete diffusivity values quoted by Neville (1995) and Tatro (2006) and therefore longer timescales than those indicated below would be required with concrete of a lower thermal diffusivity (see also Figure 12). The range of times within the shaded zones for each pile diameter in Figure 11 relate to the number of pipes installed, their size and their position. However, generally the most important factor is the size of the pile, with 1200mm diameter piles taking up to 4 days to reach a steady state compared with 300mm piles which take less than half a day (Figure 10). The larger diameter piles also have a greater range of times, with piles with smaller concrete cover taking more time to reach steady state compared with piles with centrally placed pipes.

Figure 12 shows the effect of thermal diffusivity on the time taken to reach steady state for a 1200mm diameter pile with 8 pipes installed with 75mm concrete cover. This shows that both the ground and concrete diffusivity affect the results with the effect of the concrete being the more significant. When the thermal diffusivity of both these materials is reduced from  $1.25 \times 10^{-6} \text{ m}^2/\text{s}$  to  $0.625 \times 10^{-6} \text{ m}^2/\text{s}$ , the time to achieve steady state increases from just under three days to approximately 5 days.

These results are significant as most design software uses hourly heating and cooling load timesteps. Significant changes to the heating and cooling load profiles can occur over a single day as the energy demand can differ markedly between day and night. Use of a steady state pile resistance in these cases, rather than a combined transient model of the pile and the ground, could lead to the overestimation of the temperature changes of the heat exchange fluid, especially for larger diameter piles with a highly variable thermal load. The results also suggest that the piles themselves are playing an important role in storing energy rather than just transferring it to the ground.

## 5 Pipe to Pipe Interactions

The transient pile and ground model (Section 4) overcomes important shortcomings associated with the simpler steady state pile only model (Section 3), but still cannot take into account a number of other factors that affect real heat exchangers. Most importantly, the two dimensional model cannot take into account three dimensional effects. These include the ability of the pipes to exchange heat with each other, rather than just transfer it to the concrete and ultimately the ground. This will affect the heat flow path and as a consequence the effective thermal resistance,  $R_b^*$ .

Pseudo-three dimensional models which take in account these effects have been produced for the two pipe case (eg Diao et al, 2004). As a consequence for the special two pipe case methods do exist for calculating the effective thermal resistance including pipe to pipe interactions.  $R_b^*$  is a function of both  $R_b$  and the internal resistance between the heat transfer pipes, known as  $R_a$ . For the two pipe case Hellstrom (1991), Diao et al (2004) and Lamarche et al (2010) present approaches for determining  $R_a$  and thus  $R_b^*$ . However methods are not available for multiple pipe scenarios which are more relevant for pile heat exchangers.

The magnitude of the pipe to pipe interaction effect and therefore  $R_b^*$  also depends strongly on the flow conditions within the pipes, the spacing between the pipes and the length of the pipe circuit within the ground heat exchanger (Loveridge & Powrie, 2013). The pile size, concrete and ground thermal conductivities as well as their ratio also affect the value of  $R_a$  (Hellstrom, 1991), and hence  $R_b^*$ , but to a lesser extent. In



most cases pile heat exchangers will be less susceptible to interference between the pipes than borehole heat exchangers owing to the greater separation between the pipes (typically 250 mm to 300 mm) and the much shorter length of the heat exchanger and therefore the pipe circuit. This view is supported by Anstett et al (2005) who report the influence of the internal resistance is much less than that of  $R_b$ , stating that the effect of pipe to pipe interactions can be regarded as secondary.

However, there is an increasing trend for pipes to be installed together in the centre of CFA piles and this would lead to the potential for increased interactions between the pipes. This would also cause larger errors to be associated with the application of Equation 15, which does not include for these interactions. However, due to the installation constraints of plunging the cage and the pipework into the pile concrete after pouring, it is in practice not possible to construct pile heat exchangers greater than around 20m deep by CFA techniques. This will therefore act to minimise the total amount of pipe to pipe interactions that could occur through limiting the length of the pipe circuit.

## 6 Comparison with Case Study Data

The results from four published case studies where the thermal resistances of pile heat exchangers were determined in situ from thermal response testing and/or system back analysis are summarised in Table 5. Error! Reference source not found.. Taken as a whole, the values are greater than the range for borehole heat exchangers in Table 1. As thermal response testing determines only the total resistance,  $R_b$ , it has been necessary to calculate the pipe resistance  $R_p$  (according to Equations 2 to 5) and subtract this from the total resistance in order to facilitate comparison with the results of the numerical analyses in this study.

The range of concrete resistance values estimated from the simulations described in this paper is wide, with values from 0.02 mK/W 0.3 mK/W being feasible depending on the thermal conductivity of the concrete. This is a significantly greater range than the *in situ* derived data for concrete resistance given in Table 5. In addition, the *in situ* results are skewed to the higher end of the theoretical resistance range, typically being greater than 0.1, even for multiple U-tubes. There are three possible explanations for this. First, as has already been suggested, concrete used in piling is typically at the lower end of the thermal conductivity range. Secondly, these two dimensional models do not take into account the 3D effects related to flow within the pipes and potential thermal interactions between the pipes. Finally, the available *in situ* testing dataset is very small, and in particular is skewed to the smaller pile diameters. Thus the comparison illustrates that a much greater range of case studies is required to build a reliable empirical knowledge base. Also, the level of detail associated with such case studies needs to be increased to allow proper evaluation of design approaches.

**Table 5 In situ measurements of pile thermal resistance**

Pile Type	Pile Diameter	No Pipes	Pipe Diameter	In Situ Total Thermal Resistance ( $R_b$ ) <sup>1</sup>	In Situ Concrete Resistance ( $R_c$ ) <sup>2</sup>	Source
Precast hollow concrete pile with grout in centre	0.4m	Double U-tube in series	$r_o=10\text{mm}$	0.13 mK/W	0.11 mK/W	Park et al (2013)
	0.4m	Triple U-tube in series	$r_o=10\text{mm}$	0.10 mK/W	0.09 mK/W	
continuous flight auger (CFA)	0.3 m	Single U-tube	$r_o=32\text{mm}$	0.22 mK/W <sup>2</sup>	0.11	Wood et al (2010) <sup>3</sup>
bored cast in situ	0.6 m	Single U-tube	$r_i=20\text{mm}$	0.25 mK/W	0.19	Gao et al (2008)
		Double U-tube in series		0.175 mK/W	0.15	
		Triple U-tube in series		0.15 mK/W	0.13	
square concrete driven	0.27 m	Single U-tube	$r_o=32\text{mm}$	0.17 mK/W	In sufficient data to calculate	Lennon et al (2009)
steel tubular driven; grouted inside	0.244 m	Single U-tube	$r_o=32\text{mm}$	0.11 mK/W	In sufficient data to calculate	

1. Total thermal resistance as published by the source document.
2. Concrete resistance calculated subtracting the pipe resistance (Equations 2 to 5) from the value in the previous column. Pipe numbers and sizes as per source document; turbulent flow assumed in all cases except Wood et al (2010) where flow was known to be laminar (Wood, C., 2011, Pers Comm.).
3. In situ testing was supplemented by back analysis of system behaviour.

## 7 Conclusions

Numerical models presented in this study have shown that the key controlling factors for pile concrete thermal resistance  $R_c$  are the thermal conductivity of the concrete, the number of heat exchange pipes and the amount of concrete cover to those pipes. Generally  $R_c$  will be less in cases where there are more pipes installed with less concrete cover. Therefore, to minimise the concrete resistance larger piles with many pipes near the edge of the pile should be installed. However, the benefit of additional pipes decreases as more pipes are added. Also, increasing the pipe circuit length will increase the potential for detrimental pipe to pipe interactions. CFA piles with centrally placed pipes will always have a larger resistance and will be more prone to pipe to pipe interactions. Such piles also show minimal benefit from the installation of more than two pipes.

Many simple methods for estimating thermal resistance assume that while the surface temperature of a vertical heat exchanger may vary with time, the circumferential temperature is uniform at any given time. Numerical modelling of pile heat exchangers has shown that except for CFA piles where  $r_b/c < 2$ , these methods are not applicable to pile heat exchangers.

For the special case of pile heat exchangers with only one pair of pipes installed, the validity of existing analytical approaches for determining resistance of borehole heat exchangers has been tested. It was found that the line source equation provides an

appropriate solution with a high degree of accuracy. This is because the approach accounts fully for the arrangement of the pipes as well as allowing for a spatially variable circumferential temperature. The results of the numerical models have been used to derive an empirical equation for the shape factor which allows the thermal resistance to be determined where more than two pipes are installed.

Modelling demonstrates that it may take several days for concrete in larger diameter (1.2m) pile heat exchangers to reach steady state. This means that existing design approaches which assume a steady state resistance are neglecting important thermal storage within the pile concrete. This will result in an overestimation of the temperature changes in the system. While this is conservative in terms of design, it misses opportunities to improve the efficiency of pile heat exchanger systems. Transient design methods which take account of the heat stored within the concrete would be more appropriate in these cases.

This paper only considers the 2D pile resistance  $R_b$ . The effective resistance, which includes 3D effects, will be larger in cases where significant pipe to pipe interactions occur. Additional research is required to define this effect for pile heat exchangers as existing studies are limited to two pipe cases. However, it is understood that the effective resistance additionally depends primarily on the pipe shank spacing, the fluid flow conditions and the pipe circuit length. Therefore it can be expected that pile heat exchangers will generally suffer less pipe to pipe interactions than borehole heat exchangers and therefore the effective resistance will not be significantly greater than the 2D resistance  $R_b$ . This is because of the greater shank spacing of the pipes within typical piles and the shorter length of pile heat exchangers. The exception to this would be CFA type piles which have small shank spacings.

The large range of thermal resistance values obtained from this study also highlights the urgent need for detailed and thorough case studies of pile heat exchanger behaviour. This will help to validate fully the models presented and also build an empirical knowledge base to provide confidence in design methods and parameter selection.

#### Acknowledgements

This work has been funded by Mott MacDonald and the Engineering and Physical Sciences Research Council (EP/H049010/1). The authors would also like to thank Peter Smith of Cementation Skanska for his useful discussion on construction details and Chris Wood of Roger Bullivant Ltd for information regarding in situ testing details.

## Appendix A

Thermal resistances for the heat flow between the pipes and the ground can be calculated by using a line source to represent the position of each pipe. Superposition can then be used to determine the total resistance. For the idealised scenario of two symmetrically placed pipes Hellstrom (1991) demonstrated that:

$$R_b = \frac{1}{4\pi\lambda_c} \left[ \ln\left(\frac{r_b}{r_o}\right) + \ln\left(\frac{r_b}{s}\right) + \sigma \ln\left(\frac{r_b^4}{r_b^4 - (s/2)^4}\right) \right] + \frac{1}{2} R_p \quad \text{Equation A-1}$$

where  $\sigma = \frac{\lambda_c - \lambda_{ground}}{\lambda_c + \lambda_{ground}}$

and in this case  $R_p$  is the resistance from the fluid to the material just outside the pipe for a single pipe. Hence for a pair of pipes the total resistance between the fluid and the outside of the pipe is  $\frac{1}{2} R_p = R_{pconv} + R_{pcond}$

Multi-poles are complex number derivatives of line sources. The computation required is therefore much more complicated than a line source, but otherwise the approach is similar. Full details of the multi-pole method are given in Bennet et al (1987). Multi-poles may be expressed as expansion series and a first order multi-pole solution for the case of the two symmetric pipes in a borehole is given as (Hellstrom, 1991):

$$R_b = \frac{1}{4\pi\lambda_{grount}} \left[ \beta + \ln\left(\frac{r_b}{r_o}\right) + \ln\left(\frac{r_b}{s}\right) + \sigma \ln\left(\frac{r_b^4}{r_b^4 - (s/2)^4}\right) \right] - \frac{1}{4\pi\lambda_{grount}} \left[ \frac{\frac{r_o^2}{s^2} \left\{ 1 - \sigma \left( \frac{s^4/4}{r_b^4 - (s/2)^4} \right) \right\}^2}{\frac{1+\beta}{1-\beta} + \frac{r_o^2}{s^2} \left\{ 1 + \sigma \left( \frac{s^4 r_b^4}{(r_b^4 - (s/2)^4)^2} \right) \right\}} \right] \quad \text{Equation A-2}$$

where  $\beta = 2\pi\lambda_{grount}R_p$ . This expression shows the line source method to overestimate  $R_b$  with the multipole method providing a corrective term (the second in Equation A-2) to address this. Hellstrom (1991) shows that the relative error between the two methods is typically less than 10% providing the pipe diameters are less than 40mm. Greater accuracy still can be obtained from higher order multi-poles, but the first order solution is quoted to be accurate to within 1% of the exact solution given from higher order assessments. Based on the results presented in this study, for the range of geometric parameters relevant to energy piles, the differences between the line and multi-pole methods appear much less than 1%.

### Appendix B Shape Factor Look Up Table

$r_b \backslash c$ $r_b \backslash r_o$		Pile Only Model Sf (by number of pipes)				Pile and Ground Model - Sf (by number of pipes)											
						$\lambda_c = \lambda_g$				$\lambda_c = 2\lambda_g$				$2\lambda_c = \lambda_g$			
		2	4	6	8	2	4	6	8	2	4	6	8	2	4	6	8
1.5	10	4.1666	5.0817	5.3740		4.1517	5.0691	5.3609		4.15	5.0691	5.3609		4.1537	5.0691	5.3609	
2	10	5.0653	7.1125	7.9191	8.3111	4.9964	7.0954	7.9020	8.2931	4.9774	7.0947	7.9020	8.2931	5.0164	7.0969	7.9020	8.2931
3	10	6.1242	9.9030	11.8928	12.9939	5.7806	9.8268	11.8587	12.9644	5.6801	9.8065	11.8586	12.9644	5.8868	9.8465	11.8621	12.9644
1.5	12	3.9944	4.9887	5.3146	5.4620	3.9810	4.9784	5.3022	5.4488	3.9793	4.9784	5.3022	5.4488	3.9834	4.9784	5.3022	5.4488
2	12	4.7888	6.9084	7.7790	8.2074	4.7195	6.8927	7.7627	8.1907	4.7004	6.8924	7.7627	8.1907	4.7398	6.8934	7.7627	8.1907
3	12	5.7228	9.4702	11.5459	12.7210	5.3916	9.3901	11.5116	12.6900	5.2947	9.3709	11.5077	12.6900	5.4937	9.4109	11.5146	12.6900
1.5	15	3.7901	4.8739	5.2408	5.4097	3.7761	4.8629	5.2279	5.3983	3.7741	4.8658	5.2279	5.3983	3.7785	4.8653	5.2279	5.3983
2	15	4.4759	6.6537	7.6020	8.0770	4.4072	6.6384	7.5856	8.0597	4.3873	6.6377	7.5856	8.0597	4.4262	6.6401	7.586	8.0597
3	15	5.2820	8.9524	11.1109	12.3756	4.9712	8.8725	11.0732	12.3482	4.8796	8.8526	11.0697	12.3479	5.0674	8.8935	11.07631	12.3484
1.18	20	2.7651	3.1076			2.7606	3.1024			2.7606	3.1024			2.7606	3.1024		
1.5	20	3.5407	4.7195	5.1424	5.3395	3.5285	4.7113	5.1320	5.3284	3.5268	4.7113	5.1320	5.3284	3.5314	4.7113	5.1320	5.3284
2	20	4.1134	6.3216	7.3603	7.8990	4.0485	6.3072	7.3436	7.8843	4.0302	6.3067	7.3438	7.8843	4.068	6.3096	7.3444	7.8843
3	20	4.7868	8.3161	10.5388	11.9063	4.5044	8.2366	10.5063	11.8782	4.4207	8.2167	10.502	11.8778	4.5923	8.2594	10.5102	11.8797
4	20	5.2842	9.6494	12.8239	15.0145	4.7186	9.4019	12.7291	14.9640	4.5599	9.3292	12.7052	14.9576	4.89	9.4771	12.7521	14.9721
6	20	6.0935	11.5821	16.1290	19.7006	4.9273	10.7497	15.6756	19.4678	4.638	10.5094	15.5408	19.4035	5.257	11.0062	15.8119	19.533
1.18	24	2.6903	3.0731	3.1761		2.6857	3.0679	3.1780		2.6857	3.0679	3.1780	0.0000	2.6857	3.0679	3.1780	
1.5	24	3.3923	4.6171	5.0762	5.2928	3.3798	4.6090	5.0664	5.2810	3.3782	4.6090	5.0664	5.2810	3.3828	4.6090	5.0664	5.2810
2	24	3.9062	6.1125	7.1992	7.7779	3.8446	6.0984	7.1847	7.7615	3.8266	6.098	7.1845	7.7615	3.8621	6.1008	7.1856	7.7615
3	24	4.5104	7.9359	10.1756	11.5959	4.2469	7.8595	10.1446	11.5700	4.1684	7.8395	10.1412	11.5695	4.3282	7.87971	10.1495	11.5718
4	24	4.9626	9.1490	12.2860	14.5256	4.4343	8.8998	12.1786	14.4537	4.2870	8.8289	12.1555	14.4475	4.5927	8.9724	12.2021	14.4619
6	24	5.6846	10.8745	15.2704	18.8094	4.6155	10.0871	14.8327	18.5762	4.3478	9.8587	14.7018	18.5126	4.9196	10.3279	14.9668	18.6406
1.18	30	2.5984	3.0304	3.1583	3.2145	2.5939	3.0250	3.1517	3.2074	2.5944	3.0250	3.1517	3.2074	2.5943	3.0250	3.1517	3.2074
1.5	30	3.2216	4.4885	4.9901	5.2320	3.2091	4.4795	4.9793	5.2206	3.2075	4.4799	4.9793	5.2206	3.2121	4.4804	4.9793	5.2206
2	30	3.6746	5.8618	6.9961	7.6208	3.6160	5.8480	6.9822	7.6051	3.5993	5.8475	6.9824	7.6051	3.6336	5.85	6.9831	7.6051
3	30	4.2067	7.4982	9.7375	11.2078	3.9648	7.4238	9.7042	11.1830	3.892	7.4048	9.701	11.1821	4.04	7.4454	9.7092	11.1846
4	30	4.6001	8.5625	11.6285	13.8774	4.1252	8.3359	11.5346	13.8272	3.9902	8.2686	11.5111	13.8205	4.2698	8.4064	11.5581	13.8342

		Pile Only Model Sf (by number of pipes)				Pile and Ground Model - Sf (by number of pipes)											
						$\lambda_c = \lambda_g$				$\lambda_c = 2\lambda_g$				$2\lambda_c = \lambda_g$			
$r_b \setminus c$	$r_b \setminus r_o$	2	4	6	8	2	4	6	8	2	4	6	8	2	4	6	8
6	30	5.2403	10.0877	14.2858	17.7543	4.2789	9.3579	13.8615	17.5220	4.0359	9.1446	13.7352	17.4576	4.556	9.5836	13.9917	17.5865
1.08	40	2.1187	2.3142			2.1187	2.3109			2.1187	2.3109			2.1187	2.3109		
1.18	40	2.4810	2.9725	3.1233	3.1902	2.4786	2.9679	3.1186	3.1857	2.4786	2.9679	3.1186	3.1857	2.4786	2.9679	3.1186	3.1857
1.5	40	3.0197	4.3201	4.8709	5.1621	3.0103	4.3145	4.8633	5.1375	3.0094	4.3145	4.8633	5.1375	3.0139	4.3145	4.8633	5.1375
2	40	3.4084	5.5517	6.7235	7.4060	3.3568	5.5392	6.7180	7.3928	3.3421	5.5392	6.7180	7.3928	3.3738	5.5429	6.7180	7.3928
3	40	3.8637	6.9803	9.1959	10.7041	3.6497	6.9135	9.1652	10.6809	3.5855	6.8947	9.1618	10.6809	3.7185	6.9339	9.1717	10.6809
4	40	4.1999	7.8935	10.8470	13.0906	3.7827	7.6861	10.7599	13.0453	3.6641	7.6233	10.7381	13.0391	3.9119	7.7515	10.7857	13.564
6	40	4.7457	9.1919	13.1293	16.4722	3.9106	8.5381	12.7337	16.2519	3.696	8.3446	12.6173	16.1906	4.1524	8.7414	12.8602	16.3189
8	40	5.2060	10.1992	14.8091	18.9318	3.9729	8.9974	13.9135	18.3361	3.6838	8.6651	13.6496	18.1584	4.3108	9.362	14.1942	18.5249
1.08	48	2.0745	2.2950	2.3565		2.0745	2.2916	2.3533		2.0745	2.2916	2.3533		2.0745	2.2916	2.3533	
1.18	48	2.4083	2.9333	3.0999	3.1740	2.4117	2.9288	3.0950	3.1673	2.4117	2.9288	3.0950	3.1673	2.4117	2.9288	3.0950	3.1673
1.5	48	2.9019	4.2138	4.7915	5.0873	2.8954	4.2071	4.7835	5.0790	2.8965	4.2071	4.7835	5.0790	2.8997	4.2071	4.7835	5.0790
2	48	3.2565	5.3646	6.5608	7.2651	3.2078	5.3524	6.5498	7.2524	3.197	5.3524	6.5498	7.2524	3.2285	5.3557	6.5498	7.2524
3	48	3.6709	6.6787	8.8629	10.3884	3.4718	6.6141	8.8373	10.3683	3.4141	6.5957	8.8346	10.3683	3.5393	6.6331	8.8441	10.3683
4	48	3.9763	7.5103	10.3848	12.6102	3.5919	7.3133	10.2999	12.5675	3.4825	7.2537	10.279	12.5621	3.714	7.3748	10.3257	12.5783
6	48	4.4711	8.6865	12.4618	15.7127	3.7060	8.0771	12.0882	15.4973	3.5078	7.8972	11.9758	15.4379	3.9312	8.2669	12.2063	15.5632
8	48	4.8875	9.5965	13.9807	17.9457	3.7607	8.4870	13.1391	17.3723	3.4937	8.1765	12.9005	17.201	4.0733	8.8218	13.3139	17.552
1.08	60	2.0194	2.2711	2.3422	2.3730	2.0194	2.2681	2.3389	2.3692	2.0194	2.2681	2.3389	2.3692	2.0194	2.2681	2.3389	2.3692
1.18	60	2.3220	2.8827	3.0690	3.1530	2.3221	2.8789	3.0642	3.1486	2.3221	2.8789	3.0642	3.1486	2.3221	2.8789	3.0642	3.1486
1.5	60	2.7678	4.0856	4.6919	5.0111	2.7618	4.0792	4.6850	5.0027	2.7613	4.0804	4.6850	5.0027	2.7659	4.0812	4.6850	5.0027
2	60	3.0863	5.1464	6.3570	7.0898	3.0412	5.1363	6.3470	7.0778	3.0313	5.1361	6.348	7.0778	3.0599	5.1397	6.3496	7.0778
3	60	3.4573	6.3366	8.4782	10.0104	3.2758	6.2760	8.4525	9.9913	3.2235	6.2598	8.4499	9.9913	3.3374	6.2943	8.4592	9.9955
4	60	3.7299	7.0808	9.8553	12.0469	3.3801	6.8998	9.7747	12.0029	3.2821	6.8464	9.7523	11.9965	3.4923	6.9571	9.7988	12.0134
6	60	4.1701	8.1267	11.7109	14.8426	3.4815	7.5683	11.3587	14.6350	3.3014	7.74048	11.254	14.5781	3.6849	7.4334	11.4699	14.6972
8	60	4.5394	8.9327	13.0575	16.8386	3.5297	7.9238	12.2816	16.2904	3.2871	7.6428	12.0506	16.1289	3.8119	8.2306	12.5245	16.4593

## References

- Amis, T., 2009. Energy Piles in the UK. Geodrilling International March/April 2009.
- Anstett, M., Hubbuch, M., Laloui, L., Matthey, B., Morath, M., Pahud, D., Parriaux, A., Rybach, L., Schonbachler, M., Tacher, L. & Wilhelm, J. (2005) *Utilisation de la chaleur du sol par des ouvrages de fondation et de soutènement en béton, Guide pour la conception, la réalisation et la maintenance*, Swiss Society of Engineers and Architects, Documentation D 0190.
- Banks, D., 2008. An Introduction to Thermogeology: Ground Source Heating and Cooling. Blackwell Publishing.
- Bennet, J., Claesson, J., Hellstrom, G., 1987. Multipole method to compute the conductive heat flow to and between pipes in a composite cylinder. Notes on Heat Transfer 3-1987. University of Lund, Department of Building Technology and Mathematical Physics. Lund, Sweden.
- Carmen, A.P., Nelson, R.A., 1921. The thermal conductivity and diffusivity of concrete. University of Illinois, Engineering Experiment Station, Bulletin No. 122, April 1921.
- COMSOL, 2010. Heat Transfer Module, User's Guide.
- Cote, J., Konrad, J.M., 2005. A generalized thermal conductivity model for soils and construction materials. Canadian Geotechnical Journal 42 (2), 443-458.
- Diao, N., Zeng, H. & Fang, Z., 2004 Improvements in modelling of heat transfer in vertical ground heat exchangers, HVAC&R Research, 10, 459-470.
- Gao, J., Zhang, X., Liu, J., Li, K., Yang, J., 2008. Numerical and experimental assessment of thermal performance of vertical energy piles: an application. Applied Energy 85, 901-910.
- Hellstrom, G., 1991. Ground Heat Storage, Thermal Analysis of Duct Storage Systems, Theory. Department of Mathematical Physics, University of Lund, Sweden.
- Incropera, F.P., Dewitt, D.P., Bergman, T.L., Lavine, A.S., 2007. Fundamentals of Heat and Mass Transfer, Sixth Edition. Hoboken, New Jersey, John Wiley & Sons.
- Khan, M.I., 2002. Factors affecting the thermal properties of concrete and applicability of its prediction models. Building and Environment 37, 607 – 614.
- Kim, K-H., Jeon, S-E., Kim, J-K., Yang, S., 2003. An experimental study on thermal conductivity of concrete. Cement and Concrete Research 33, 363 – 371.
- Lamarche, L., Kaji, S., Beauchamp, B., 2010. A review of methods to evaluate borehole thermal resistance in geothermal heat pump systems. Geothermics 39, 187-200.
- Lennon, D.J., Watt, E., Suckling, T.P., 2009 Energy piles in Scotland, in: Van Impe & Van Impe (eds), Proceedings of the Fifth International Conference on Deep

Foundations on Bored and Auger Piles. Frankfurt, 15 May 2009, Taylor & Francis Group, London.

Loveridge, F.A., Powrie, W., 2013. Pile heat exchangers: thermal behaviour and interactions, *Proceedings of the Institution of Civil Engineers Geotechnical Engineering*, 166(2), 178-196.

Neville, A.M., 1995. *Properties of concrete*, 4<sup>th</sup> edition. Longman, London.

Pahud, D., 2007. PILESIM2, Simulation Tool for Heating/Cooling Systems with Heat Exchanger Piles or Borehole Heat Exchangers, User Manual. Scuola Universitaria Professionale della Svizzera Italiana, Lugano, Switzerland.

Park, H., Lee, S-R., Yoon, S. & Choi, J-C., 2013 Evaluation of thermal response and performance of PHC energy pile: Field experiments and numerical simulation, *Applied Energy*, 103, 12-24.

Remund, C.P., 1999. Borehole thermal resistance: laboratory and field studies. *ASHRAE Transactions* 105 (1), 439-445.

Sanner, B., Hellstrom, G., Spitler, J., Gehlin S.E.A., 2005. Thermal Response Test – Current Status and World-Wide Application, in: *Proceedings World Geothermal Congress*, 24-29<sup>th</sup> April 2005 Antalya, Turkey. International Geothermal Association.

Sharqawy, M.H., Mokheimer, E.M., Badr, H.M., 2009. Effective pipe-to-borehole thermal resistance for vertical ground heat exchangers. *Geothermics* 38, 271-277.

Shonder, J.A., Beck, J.V., 2000. Field test of a new method for determining soil formation thermal conductivity and borehole resistance, *ASHRAE Transactions* 106 (2000) (1), pp. 843–850.

Tatro, S.B., 2006. Thermal properties, in: Lamond, J., Pielert, J. (eds), *Significance of tests and properties of concrete and concrete making materials*. Portland Cement Association, Stokioie, Illinois, USA.

Wood, C.J., Liu, H., Riffat, S.B., 2010 Comparison of a modeled and field tested piled ground heat exchanger system for a residential building and the simulated effect of assisted ground heat recharge. *International Journal of Low Carbon Technologies* 5, 137-143.

Yavuzturk, C., & Spitler, J.D., 1999. A short time step response factor model for vertical ground loop heat exchangers. *ASHRAE Transactions* 105 (2), 475-485.



## Figure Captions

**Figure 1 Typical Thermal Pile Construction Details; a) pipes fixed to a rotary bored pile reinforcement cage; b) contiguous flight auger pile with central heat exchanger pipes.**

**Figure 2 Schematic of 2D heat transfer model; a) generalised pile only geometry; b) eccentric cylinder validation geometry**

**Figure 3 Results of pile only model for 600mm diameter pile with 25mm diameter OD pipes; a) effect of number of pipes and concrete cover; b) effect of pipe positioning for CFA piles ( $c=255\text{mm}$ )**

**Figure 4 Thermal resistance comparison for different diameter piles with an overall equivalent diameter of soil and concrete of 1200mm. For the case of 25mm diameter pipes and concrete and ground conductivity of 2W/mK. a) pipes installed with 75mm concrete cover; b) pipes installed centrally in a CFA pile around a 40mm steel bar**

**Figure 5 Comparison of 2 pipe pile only model with analytical solutions (for the case of a 600mm diameter pile with 25mm diameter pipes)**

**Figure 6 Effect of ground thermal conductivity on asymptotic Shape Factor determined from transient analysis with pile and ground model (600mm diameter pile with two 25mm diameter OD pipes)**

**Figure 7 Temperature changes around the pile circumference at steady state for a 600mm diameter pile with 25mm diameter OD pipes; a) with two pipes showing the effect of concrete cover; b) with 50mm concrete cover showing the effect of the number of pipes**

**Figure 8 Difference in shape factor values between the pile only and the extended pile and ground models at steady state conditions. Multiple points plotted for each value of  $r_b/c$  corresponding to different  $r_b/r_o$  ratios.**

**Figure 9 Errors in determining  $R_c$  when using the shape factor equation (Equation 15) compared with numerical simulation; a) 2 pipes; b) 4 pipes; c) 6 pipes; d) 8 pipes.**

**Figure 10 Comparison of Pile Thermal Resistance Calculated by Equations 2, 3, 5 & 15 compared with the Multipole Simulations of Anstett et al, 2005.**

Case assessed: concrete thermal conductivity 1.8 W/mK and laminar flow in fluid. For piles less than 0.5m diameter  $r_i=8\text{mm}$ ,  $r_o=10\text{mm}$  and  $c=50\text{mm}$ . For piles greater than 0.5m diameter  $r_i=13\text{mm}$ ,  $r_o=16\text{mm}$  and  $c=100\text{mm}$  (Anstett et al, 2005).

**Figure 11 Range of Times for Pile Concrete to Reach Steady State ( $\alpha=1.25 \times 10^{-6} \text{ m}^2/\text{s}$ )**

**Figure 12 Effect of thermal diffusivity on time taken for the pile concrete to achieve steady state (1200mm diameter pile, 8 pipes, 75mm concrete cover)**